

Title	Studies on the chipboard : Part 1. Mechanical Properties
Author(s)	MAKU, Takamaro; HAMADA, Ryozo
Citation	木材研究 : 京都大學木材研究所報告 (1955), 15: 38-52
Issue Date	1955-09
URL	<a href="http://hdl.handle.net/2433/52814">http://hdl.handle.net/2433/52814</a>
Right	
Type	Departmental Bulletin Paper
Textversion	publisher

# Studies on the chipboard

## Part 1. Mechanical Properties

by Takamaro MAKU and Ryozo HAMADA

This report is on the results of studies on the mechanical properties of the chipboard and on the bending strength of chipboard beam.

### I. Experimental procedure

#### 1. Panel preparation

The wood particles used in this experiment are divided into the following 2 basic types.

S-type : 5 cm long, 1.3 mm wide, and 0.28, 0.61, or 1.18 mm thick, shaved from beech veneer of 1.3 mm thick.

R-type : 5 cm long, 1.2 cm wide, and 0.24 mm thick, shaved from 1.2 cm thick lumber of Japanese cypress.

The weight of urea resin applied was 7.3 % of particles in S-type and 6.5 % in R-type, then the particles were conditioned to about 12~13% moisture content and hot pressed in the range of specific gravity 0.4~1.1.

#### 2. Types of Tests.

Measurements were made for the determination of (a) specific gravity, (b) moisture content, (c) tensile and compressive strength, (d) modulus of elasticity in tension and compression, and (e) shearing strength.

The testing pieces are shown in Fig. 1.

### II. Mechanical properties of chipboard

#### 1. Strength-density relation

The relations between the specific gravity and the tensile-, compressive-, and shearing-strength of the chipboard (S-type) are shown in Fig. 2 and these results illustrate the same relation as in wood. As for these relations, there are few reports hitherto KOLLMANN<sup>1)</sup> indicates an exponential curve and TURNER<sup>2)</sup> an linear relation between the modulus of rupture and specific gravity.

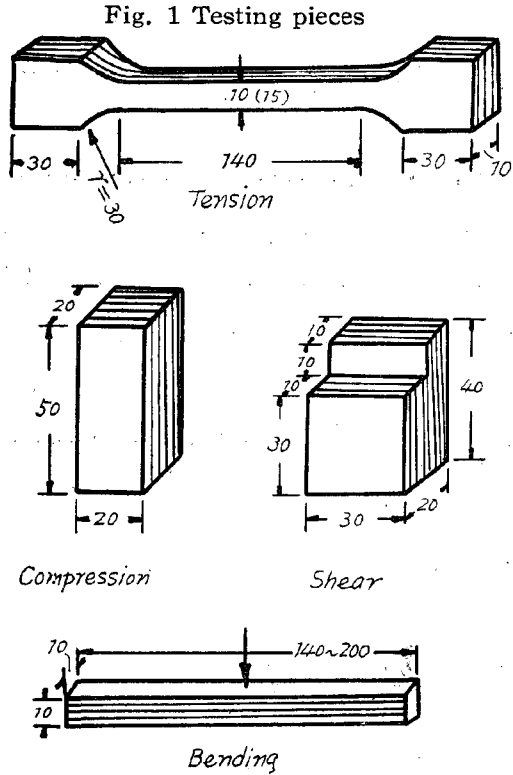
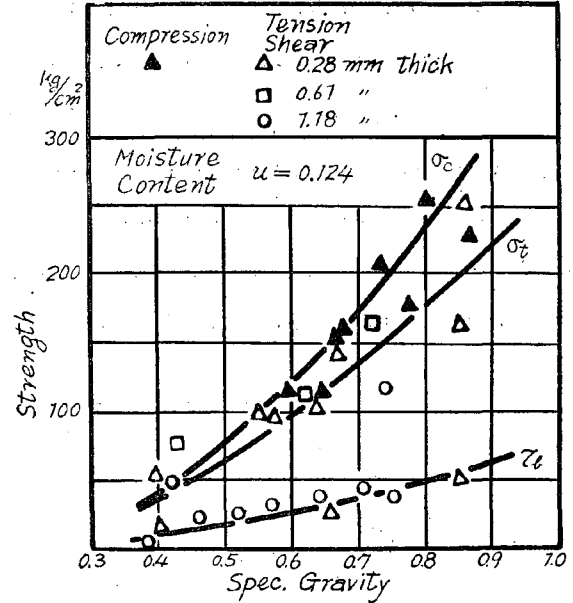


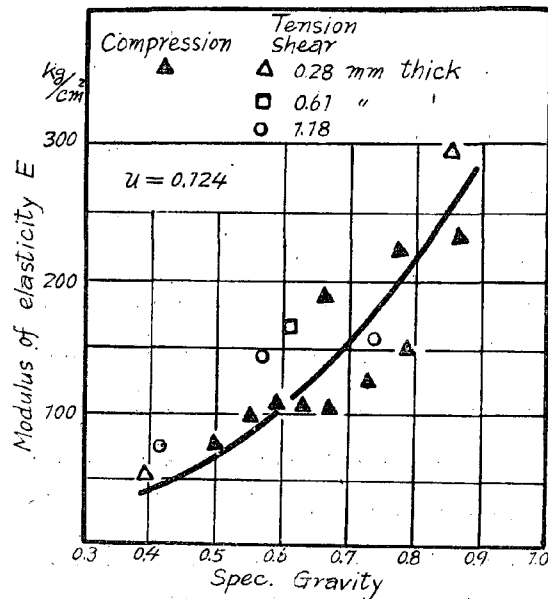
Fig. 2 The relation of tensile, compressive, and shearing strength to specific gravity



As for the effect of the thickness of particles on the strength of chipboard, the influences were scarcely found at least in this experiment as clearly shown in Fig. 2. In regard to this relation, TURNER also obtained the same result on a certain particle.

The relation between the elastic modulus and the specific gravity is shown in Fig. 3.

Fig. 3 The relation of elastic modulus to specific gravity



In the Figure,  $E_t$  seems to be a little larger than  $E_c$  as same as in wood ( $E_t, E_c$  : elastic

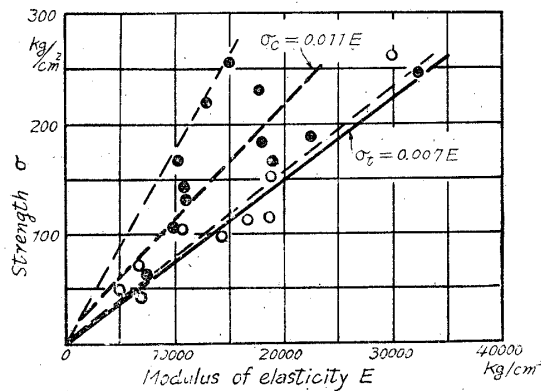
modulus in tension and compression), but they can be regarded equal and the relation is shown also in exponential curve.

For the chipboard of R-type or leaf-like shavings, the quite same conclusion seems to be given except that there is a considerable difference between  $E_t$  and  $E_c$  in R-type chipboard of spec. gravity 0.7 and over. It is noteworthy and important in practise that the tensile strength  $\sigma_t$  is smaller than compressive strength  $\sigma_c$ .

### 2. Strength-elastic modulus relation

From above results the relations between  $\sigma_t$  and  $E$ ,  $\sigma_c$  and  $E$  are given as follows in moisture content  $u=0.124$  (see Fig. 4).

Fig. 4 The relation of tensile and compressive strength to elastic modulus



$$\left. \begin{aligned} \sigma_t &= 0.007 E \\ \sigma_c &= 0.011 E \end{aligned} \right\} \dots\dots\dots (1)$$

### III. Bending failure of chipboard beam

#### 1. Stress-strain curve

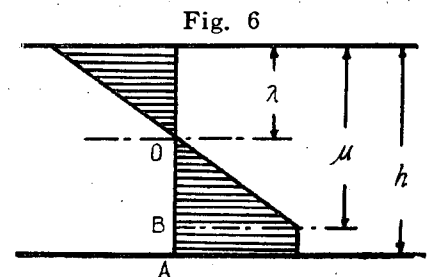
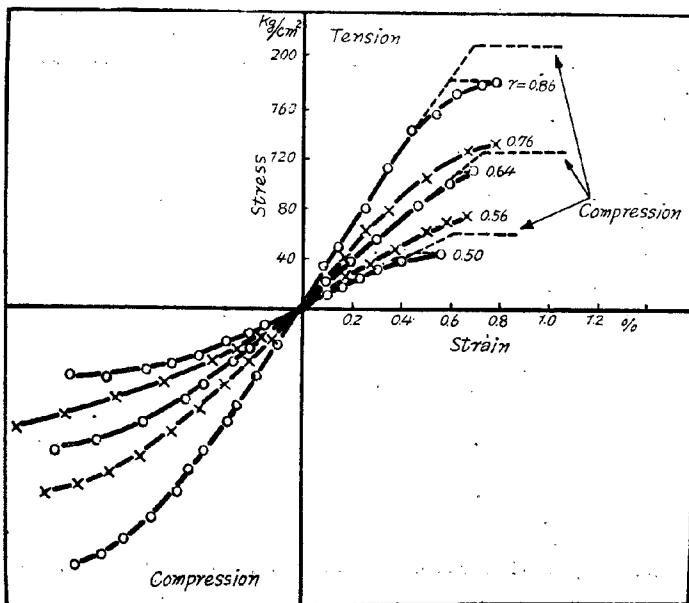
The typical stress-strain curves of chipboard are, as shown in Fig. 5, similar to that of wood. However, as mentioned above, there is observed characteristics that the tensile strength is smaller than the compressive strength, and in soft- and semi-hard-chipboard which is of most practical use, when the tensile stress reaches to the ultimate strength the compressive stress yet remains within the proportional limit, while in hard chipboard the compressive stress reaches barely to plastic region when the tensile stress reaches to the ultimate strength. In this figure the simplified stress-strain curves are shown as dotted lines.

As for R-type the same matter can be explained except that in semi-hard and hard board the slope of stress-strain curve in tension differs, as above mentioned, from that in compression, but the following discussion are made under the simplification of  $E_t = E_c$ .

2. Single section beam

As for the condition of bending failure of wood beam, KON<sup>3)</sup>, SAWADA<sup>4)</sup> and the others published the reports in consideration of plastic region. On chipboard-beam, as obvious from Fig. 5, the authors present the stress distribution in which there exists the plastic region only in the tension side in cross section (Fig. 6) and this stress distribution just coincides with the KON's one when the tension and compression side are exchanged. So,

Fig. 5 Stress-strain curves of chipboard of specific gravity 0.50, 0.56, 0.64, 0.74, and 0.86



with exception of a few incidental conditions, one can obtain the bending failure coefficients in the similar way as in KON's case.

For instance, in a simple beam which supports a concentrated center load.

*Bending failure coefficient (caused by tension) in plastic region  $\sigma_b$*

$$\sigma_b = \frac{3r-1}{r+1} \sigma_t \dots\dots\dots (2)$$

were  $r = \sqrt{\frac{2-K}{K}}$ ,  $K = OB/OA$  in Fig. 6.

*Bending failure coefficient (caused by horizontal shear) in plastic region  $\sigma_{sb}$*

$$\left. \begin{aligned}
 p\sigma_b &= \frac{3\sigma_t}{1 + \frac{\sigma_t}{\tau_b} \frac{h}{l}} \\
 \text{or } \tau_b &= \frac{\sigma_t}{3 \frac{\sigma_t}{p\sigma_b} - 1} \frac{h}{l}
 \end{aligned} \right\} \dots\dots\dots (3)$$

where  $\tau_b$  is shearing strength of chipboard,  $l$  span and  $h$  height of section.

*Bending failure coefficient (caused by horizontal shear) in elastic region  $e\sigma_b$*

$$\left. \begin{aligned}
 e\sigma_b &= \frac{2\tau_b}{\frac{h}{l}} \\
 \text{or } \tau_b &= \frac{e\sigma_b}{2} \frac{h}{l}
 \end{aligned} \right\} \dots\dots\dots (4)$$

Then, the critical value of  $h/l$  between eq. (2) and (3), i.e.  $(h/l)_1$ , and that between eq. (3) and (4) i.e.  $p(h/l)_e$  is given as follows.

$$\left. \begin{aligned}
 (h/l)_1 &= \frac{4}{3r-1} \frac{\tau_b}{\sigma_t} \\
 p(h/l)_e &= \frac{2\tau_b}{\sigma_t}
 \end{aligned} \right\} \dots\dots\dots (5)$$

thus      for     $h/l < (h/l)_1$                       eq. (2) is applicable  
             for     $(h/l)_1 < h/l < p(h/l)_e$             eq. (3)        "  
             for     $h/l > p(h/l)_e$                       eq. (4)        "

Table 1 gives the illustrations of bending test pieces. According to this table, in all test pieces  $h/l$  is smaller than  $(h/l)_1$ , namely, the bending failure must be caused by tensile failure (eq. (2)) and this coincides well with the result of actual bending test.

Table 1

Type	spec. gravity	$\sigma_t$	$\tau_b$	$K$	$h$	$l$	$h/l$	$(h/l)_1$	$p(h/l)_e$	$\sigma_b$
S	0.51	63	18	0.93	1.13	12	0.0946	0.514	0.572	67
	0.61	105	26	0.75	1.13	16	0.0706	0.349	0.495	131
	0.74	155	38	0.89	1.21	16	0.0756	0.414	0.49	175
	0.86	208	58	0.63	1.16	16	0.0726	0.351	0.558	276
R	0.6	85	23	0.68	0.98	12	0.0817	0.345	0.54	117

The value of  $h/l$  in practical use is regarded generally to be smaller than that of this experiment, therefore it is enough to be expected that the bending failure is caused mainly by the tension failure.

3. 3-ply composite section (all chipboard)

As for the bending failure of the laminated wood beam (3-ply), MORI, ASANO<sup>5)</sup> and SAWADA<sup>6)</sup> have reported their studies.

To extend the stress-strain relation from single section to composite one is somewhat doubtful and, in general, with increase of the plastic region the stress distribution in composite section which is only geometrical superposition of that in single section shall lose its accuracy. But in this report the authors will use this distribution as an approximation.

The process of the stress distribution of this case can be divided in many cases, but from eq. (1)

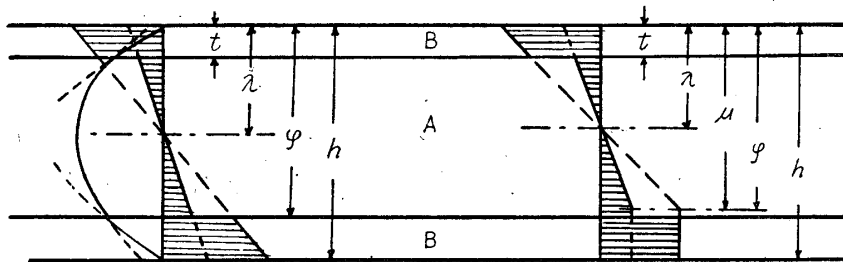
$$\frac{\sigma_{tA}}{\sigma_{tB}} = \frac{0.007 E_A}{0.007 E_B} = \frac{E_A}{E_B}$$

$$\therefore n = e \dots\dots\dots(6)$$

Where  $E_A, E_B$  is elastic modulus of core A and face B,  $\sigma_{tA}, \sigma_{tB}$  is tensile strength of those, and  $n = \sigma_{tA}/\sigma_{tB}, e = E_A/E_B$ .

And in practise the bending failure of beam is mainly caused by the tension failure of skin of tension side, so the process of stress distribution in Fig. 7 becomes important.

Fig. 7



This case is almost the same as SAWADA's case with the exception of few incidental conditions when its tension side and compression side are replaced. Therefore in the the similar way as in SAWADA's case, the following modulus of rupture  $\sigma$  are obtained in the beam under a concentrated center load. (in such a kind of construction the maximum shearing stress takes place in the compression side of core A because the ratio  $t/\mu$  is comparatively small)

*Bending failure coefficient (caused by tension) in plastic region  $\sigma_b$*

$$\sigma_b = \frac{\sigma_{tB}}{e} \left[ 3a_0 - 2\gamma_0(\mu_0 + 2t_0) + \frac{4t_0\gamma_0\mu_0^2}{\mu_0^2 - (1-e)(\mu_0 - t_0)^2} \right] \dots\dots\dots(7)$$

$$a_0 = e(1 - \varphi_0 + n\varphi_0^2) + (1-e)nt_0^2$$

$$\gamma_0 = e(1 - \varphi_0 + n\varphi_0) + (1-e)nt$$

$$\mu_0 = \frac{B}{eA} \left[ -1 + \sqrt{1 - 2e\frac{A}{B} - e(1-e)(2-t_0)t_0\left(\frac{A}{B}\right)^2} \right]$$

$$A = n(1-K)$$

$$B = e(1 - \varphi_0 + n\varphi_0)K + (1-e)nt_0$$

$$t_0 = t/h$$

$$\varphi_0 = \varphi/h$$

*Bending failure coefficient (caused by horizontal shear) in plastic region  ${}^p\sigma_b$*

$$\left. \begin{aligned} {}^p\sigma_b &= \frac{2\tau_b}{(h/l)h} \theta_1 \\ \text{or } \tau_b &= \frac{{}^p\sigma_b(h/l)h}{2\theta_1} \end{aligned} \right\} \dots\dots\dots(8)$$

$$\theta_1 = \frac{h}{2} \{e\mu_0 + (1-e)t_0\} \left[ 1 - \frac{4t_0^2(1-e)(\mu_0 - t_0)\mu_0}{\{\mu_0^2 - (1-e)(\mu_0 - t_0)^2\}^2} \right]$$

$\mu_0$  : that of eq. (7)

*Bending failure coefficient (caused by horizontal shear) in elastic region  ${}^e\sigma_b$*

$$\left. \begin{aligned} {}^e\sigma_b &= \frac{2\tau_b}{(h/l)h} \beta_0 \\ \tau_b &= \frac{{}^e\sigma_b(h/l)h}{2\beta_0} \end{aligned} \right\} \dots\dots\dots(9)$$

$$\beta_0 = h\phi_0/2\{e\lambda_0^2 + (1-e)(2\lambda_0 - t_0)t_0\}$$

$$\phi_0 = 2\{1 - (1-e)(\varphi_0^3 - t_0^3)\} - 3\{1 - (1-e)(\varphi_0^2 - t_0^2)\}\lambda_0$$

The critical  $h/l$  of eq. (7) and (8) (that is  $(h/l)_1$ ) is

$$(h/l)_1 = \frac{2\tau_b}{h\sigma_b} \theta_1 \dots\dots\dots(10)$$

The requirement of the critical value of  $h/l$  between eq. (8) and (9) i.e.  ${}^p(h/l)_e$  is complicated in calculation and may be unnecessary in practise, so it is abridged in this report. In addition, the shearing stress in glue line comes into question in general but for soft or semi-hard chipboard core it can be neglected.



The illustration of this case is given about the following construction. (Table 2)

Table 2

Type		$\sigma_{tB}$	$\tau_A$	$e$	$n$	$K$	$h$	$\varphi_0$	$t_0$	$l$	$h/l$	$(h/l)_1$
1	spec. grav. core 0.4 face 0.74	150	11	0.29	0.27	0.7	1.64	0.8	0.195	18	0.091	0.120
2	core 0.58 face 0.74	150	23	0.63	0.60	0.70	1.59	0.8	0.201	18	0.088	0.162

According to Table 2, in both of type 1 and 2 the bending failure must be caused by the tension failure of skin of tension side. But as a matter of fact, in type 1 whose core is small shearing strength the failure is evidently caused by the horizontal shear. This discrepancy may be caused by lack of uniformity of core or, as has been previously mentioned, by the error rised from simple geometrical combination of the stress distributions of the single section.

#### 4. 3-ply composite section (veneer-overlay)

This case is most important in practice, and first, the authors must find the relations between  $\sigma_t$  and  $E$ ,  $\sigma_c$  and  $E$  in order to determine the basic form of the stress distribution. That is,

$$\begin{aligned} \text{for air dried wood} & \begin{cases} \sigma_c = 0.003 \sim 0.004E \doteq 0.0035E \\ \sigma_t \doteq 2\sigma_c = 0.007E \end{cases} \\ \text{for chipboard} & \begin{cases} \sigma_c = 0.011E \\ \sigma_t = 0.007E \end{cases} \end{aligned}$$

then

$$\begin{aligned} \frac{\sigma_{tA}}{\sigma_{tB}} &= \frac{0.007E_A}{0.007E_B} = \frac{E_A}{E_B}, & \therefore n &= e \\ \frac{\sigma_{cA}}{\sigma_{cB}} &= \frac{0.011E_A}{0.0035E_B} \doteq 3 \frac{E_A}{E_B} & \therefore p &= 3e \quad (p = \sigma_{cA}/\sigma_{cB}) \end{aligned}$$

So, in tension side, both the elastic limits of core and face veneer exist in a same plane and in compression side plastic region of the face veneer proceeds that of core, then the following 2 process of stress distribution are expected (Fig. 8).

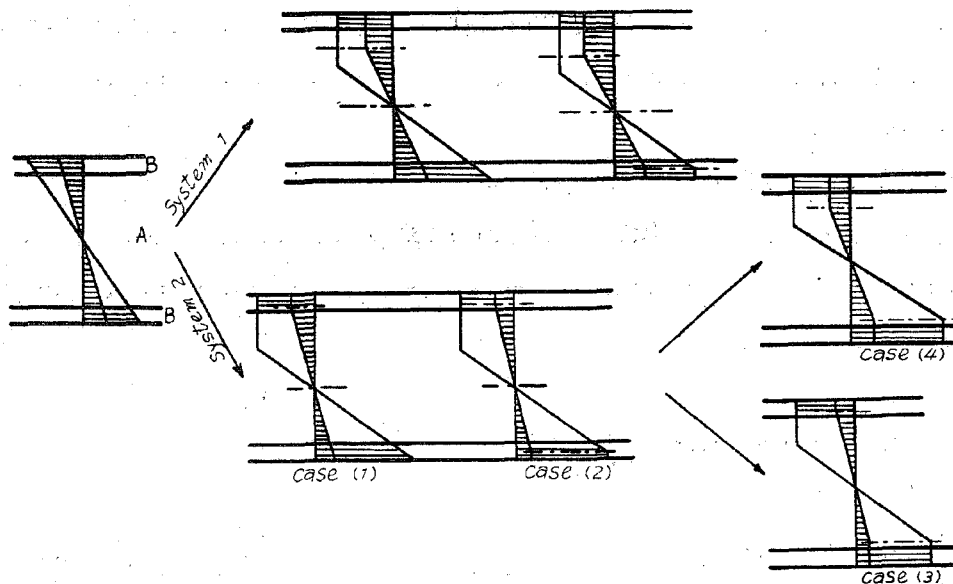
System 1. for soft board (of low shearing strength), overlaid by veneer of every kind of thickness or for semi-hard board overlaid by veneer of comparatively thick.

System 2. for semi-hard board overlaid by veneer of comparative thinn.

This classification is based on the results of Fig. 2 and 3, but in such a chipboard where the strength is large for its specific gravity, the "System 1" transfer to the "System 2", so the "System 2" becomes important. (The solutions for System 1 are quite same as SAWADA'S solutions for laminated wood beams)

As the requirement of the curve of the horizontal shearing stress distribution is troublesome in this section and in the beam whose core has the comparatively large shearing strength, it can be considered that the bending failure is caused mainly by the tension failure of skin, so, hereafter, the authors shall search about the bending failure by tension failure excepting case (1) in Fig. 8.

Fig. 8



As there are hardly reported about the value of  $K$  in tension of veneer, the authors obtained  $K=0.9$  for some species, therefore it is expected that the case (1) and (2) in Fig. 8. come up most frequently in practise.

**a. In elastic region (Fig. 9)**

From horizontal forces  $\sum H=0$  in Fig. 9<sup>(3), (6)</sup>

$$\lambda = \frac{h^2 - (1-e)(\varphi^2 - t^2)}{2\{h - (1-e)(\varphi - t)\}}$$

$$\lambda_0 = \frac{\lambda}{h} = \frac{1 - (1-e)(\varphi_0^2 - t_0^2)}{2\{1 - (1-e)(\varphi_0 - t_0)\}}$$

$$\frac{M}{W} = \frac{4\{1 - (1-e)(\varphi_0^3 - t_0^3)\}\{1 - (1-e)(\varphi_0 - t_0)\} - 3\{1 - (1-e)(\varphi_0^2 - t_0^2)\}^2}{1 - (1-e)(\varphi_0 - t_0)(2 - \varphi_0 - t_0)} \sigma_2$$

where  $M$  is the bending moment and  $W$  is section modulus. At the extreme  $\sigma_2 = \sigma_{cB}$ , so the bending stress  $\sigma_{be}$  is

$$\sigma_{be} = \frac{4\{1-(1-e)(\varphi_0^3 - t_0^3)\}\{1-(1-e)(\varphi_0 - t_0)\} - 3\{1-(1-e)(\varphi_0^2 - t_0^2)\}^2}{1-(1-e)(\varphi_0 - t_0)(2 - \varphi_0 - t_0)} \sigma_{cB} \dots\dots\dots(11)$$

Maximum shearing stress  $\tau_m$  in core A is

$$\tau_m = \frac{3Q}{2b} \frac{1}{\frac{h\phi_0}{2\{e\lambda_0^2 + (1-e)(2\lambda_0 - t_0)t_0\}}} = \frac{3Q}{2b\beta_0} \dots\dots\dots(12)$$

$$\phi_0 = 2\{1-(1-e)(\varphi_0^3 - t_0^3)\} - 3\{1-(1-e)(\varphi_0^2 - t_0^2)\}\lambda_0$$

$$\beta_0 = \frac{h\phi_0}{2\{e\lambda_0^2 + (1-e)(2\lambda_0 - t_0)t_0\}}$$

$Q$  : shearing force

$b$  : width of section

Fig. 9

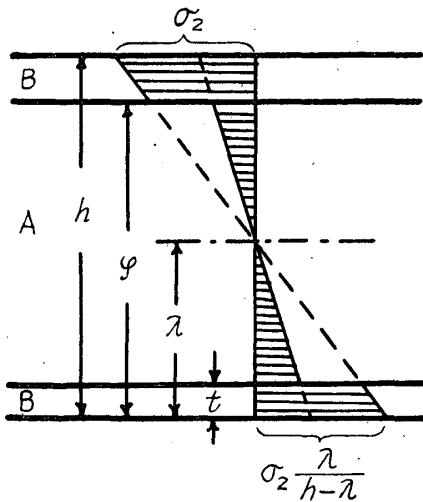
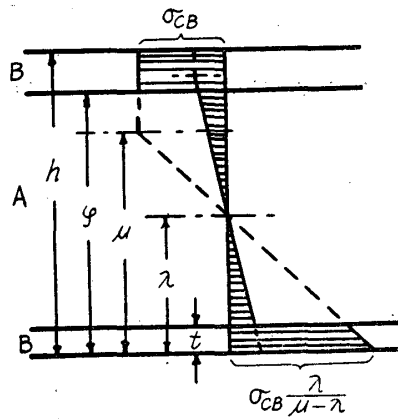


Fig. 10



**b. In plastic region**

case 1. (Fig. 10)

From Fig. 10 similarly

$$\lambda_0 = \frac{2(1-\varphi_0)\mu_0 + e\varphi_0^2 + (1-e)t_0^2}{2\{(1-\varphi_0 + e\varphi_0) + (1-e)t_0\}}$$

$$\mu_0 = \frac{2\{(1-\varphi_0 + e\varphi_0) + (1-e)t_0\}\lambda_0 - \{e\varphi_0^2 + (1-e)t_0^2\}}{2(1-\varphi_0)} \dots\dots\dots(a)$$

$$\frac{M}{W} = \sigma_{cB}(1-\varphi_0) \left\{ 3(1+\varphi_0) - \frac{6B\lambda_0 - 4C}{2A\lambda_0 - B} \right\} \dots\dots\dots(b)$$

$$A = e\varphi_0 + (1-e)t_0$$

$$B = e\varphi_0^2 + (1-e)t_0^2$$

$$C = e\varphi_0^3 + (1-e)t_0^3$$

at the extreme  $\sigma_{eB} \frac{\lambda}{\mu - \lambda} = \sigma_{tB}$

then  $\mu_0 = (1+m)\lambda_0 \quad (m = \sigma_{eB}/\sigma_{tB}) \dots\dots\dots (c)$

from eq. (a), (c)

$$\lambda_0 = -\frac{e\varphi_0^2 + (1-e)t_0^2}{2(m - m\varphi_0 - e\varphi_0) - (1-e)t_0} \dots\dots\dots (d)$$

using this  $\lambda_0$ , the bending failure coefficient (caused by tension)  $\sigma_b$  becomes from eq.

(b)

$$\sigma_b = \sigma_{eB}(1-\varphi_0) \left\{ 3(1+\varphi_0) - \frac{6B\lambda_0 - 4C}{2A\lambda_0 - B} \right\} \dots\dots\dots (13)$$

, ( $\lambda_0 =$  eq. (d))

and maximum shearing stress  $\tau_m$  in core A is

$$\tau_m = \frac{3Q}{2b\psi_0}$$

$$\psi_0 = \frac{(3B^2 - 4AC)Ah}{4\{e\{2(1-\varphi_0) + A\}\lambda_0^2 + [2(1-e)t_0\{(1-\varphi_0) + A\} - 2e\mu_0(1-\varphi_0)]\lambda_0 - (1-e)\{t_0^2A + 2\mu_0t_0(1-\varphi_0)\}\}A + e(2A\lambda_0 - B)^2} \dots\dots\dots (14)$$

, ( $\lambda_0 =$  eq. (d))

then, under a concentrated center load

*Bending failure coefficient (caused by horizontal shear)  $\nu\sigma_b$*

$$\left. \begin{aligned} \nu\sigma_b &= \frac{2\tau_b}{(h/l)h} \psi_0 \\ \text{or } \tau_b &= \frac{\nu\sigma_b(h/l)h}{2\psi_0} \end{aligned} \right\} \dots\dots\dots (15)$$

*Bending failure coefficient (caused by horizontal shear) in elastic region* is from eq. (12)

$$\left. \begin{aligned} e\sigma_b &= \frac{2\tau_b}{(h/l)h} \beta_0 \\ \tau_b &= \frac{e\sigma_b(h/l)h}{2\beta_0} \end{aligned} \right\} \dots\dots\dots (16)$$

The critical value  $(h/l)_1$  between eq. (13) and (15) is given

$$\left(\frac{h}{l}\right)_1 = \frac{2\tau_b}{\sigma_b h} \psi_0 \dots\dots\dots (17)$$

**case 2 (Fig. 11)**

*Bending failure coefficient (caused by tension) in plastic region*

$$\sigma_b = \sigma_{tB} \left[ 3m(1-\varphi_0)(1+\varphi_0-2\lambda_0) + (3-K^2)\lambda_0^2 + \frac{2}{K\lambda_0} \{e(\varphi_0-\lambda_0)^3 - (1-e)(\lambda_0-t_0)^3\} \right] \dots\dots\dots (18)$$

$$\lambda_0 = \frac{B}{A} \left[ -1 + \sqrt{1 - \{(1-e)t_0^2 + e\varphi_0^2\} \frac{A}{B^2}} \right]$$

$$A = (1-K)^2$$

$$B = \{(m-m\varphi_0)K - e\varphi_0 - (1-e)t_0\}$$

Fig. 11

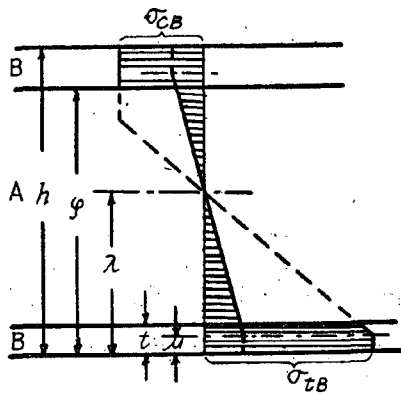
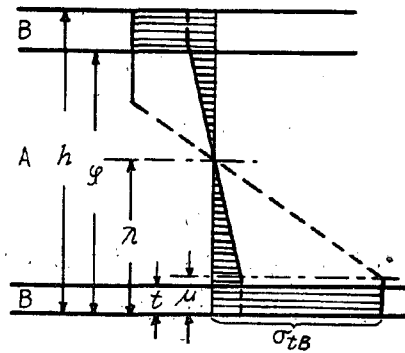


Fig. 12



**case 3 (Fig. 12)**

*Bending failure coefficient (caused by tension) in plastic region*

$$\sigma_b = \sigma_{tB} \left[ 3m(1-\varphi_0)(1+\varphi_0-2\lambda_0) + e\{3(\lambda_0-t_0)^3 - K^2\lambda_0^2\} + \frac{2}{K\lambda_0} (\varphi_0-\lambda_0)^3 \right] \dots\dots\dots (19)$$

$$\lambda_0 = \frac{B}{A} \left[ -1 + \sqrt{1 - e\varphi_0^2 \frac{A}{B^2}} \right]$$

$$A = e(1-K)^2$$

$$B = \{(m-m\varphi_0) - e\varphi_0 - (1-e)t_0\}$$

case 4 (Fig. 13)

*Bending failure coefficient (cause by tension) in plastic region*

$$\sigma_b = \sigma_{tB} \left( 3m(1 - \varphi_0^2 + p\varphi_0^2) - 6m\{(1 - \varphi_0 + p\varphi_0) - (1 - e)t_0\}\lambda_0 - [3e(\omega + 1) - eK^2\{\omega + 1\}^2 + (\omega - 1)(\omega - 2)]\lambda_0^2 \right) \dots \dots \dots (20)$$

$$\lambda_0 = \frac{2\{m(1 - \varphi_0) - (1 - e)t_0\}}{2(\omega + 1)\{2 + (\omega - 1)K\}}$$

$$\omega = pm/e, \quad p = \sigma_{cA}/\sigma_{cB}, \quad m = \sigma_{cB}/\sigma_{tB}$$

$$\mu_{10} = (1 - K)\lambda_0, \quad \mu_{20} = (1 + \omega K)\lambda_0, \quad \mu_{1,20} = \mu_{1,2}/h$$

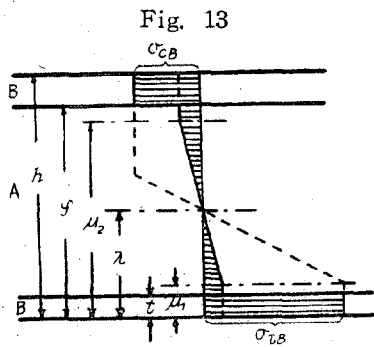


Fig. 14 Increase of modulus of rupture by 0.5, 1.0 and 1.5 mm thick veneer overlay

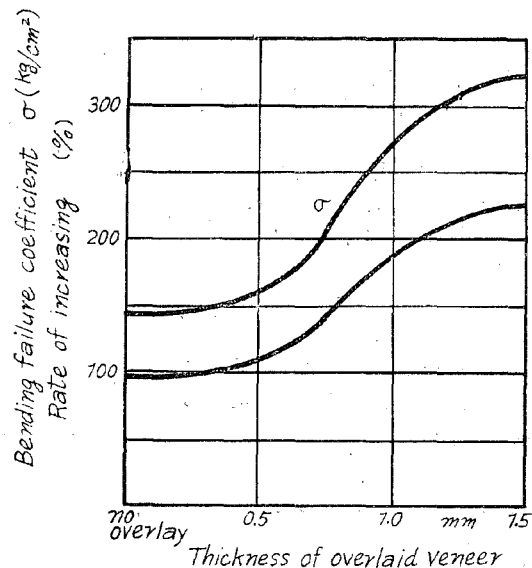


Fig. 14 is the comparison of the strength by eq. (18) or (19) when 2 cm thick chipboard core of specific gravity 0.65 is overlaid by beech veneer of 0.5, 1.0 and 1.5 mm thick respectively.

As obvious from the figure for this kind of chipboard the veneer overlay of 1~1.5 mm thick is most effective in the standpoint of bending strength, the thinner one is ineffective and the thicker is uneconomical and the bending failure caused by horizontal shearing failure may often appear in the latter.

Summary

These experiments were performed to find the relation between the mechanical pro-

perties and the specific gravity in chipboard panels made from the particles of S-type (5 cm long, 1.3 mm wide and 0.28, 0.61 or 1.18 thick) and R-type (5 cm long, 1.2 cm wide and 0.24 mm thick) and to obtain the bending failure coefficient of chipboard beam of single section, and sandwich construction.

1. The relations of tensile-, compressive-, and shearing-strength, and elastic modulus to specific gravity are shown as exponential curves (Fig. 2, 3)
2. The elastic modulus in tension and compression is nearly equal but there is characteristics that the tensile strength is comparatively smaller than the compressive strength and experimentally linear formulas (1) are estimated between tensile, compressive strength  $\sigma_t$ ,  $\sigma_c$  and elastic modulus  $E$ .
- e. The coefficients of bending failure caused by tension-, or shearing failure were determined as eq. (2), (3) and (4) for chipboard beam of single section, eq. (7), (8) and (9) for 3 ply composite section and eq. (13), (15), (16) and (18)~(20) for veneer overlaid sandwich section.

### Literature cited

- 1) Kollmann, F. : Holz als Roh- und Werkstoff 10, 12 (1952)
- 2) Turner, H. D. : J. For. Prod. Res. Soc. 6, 5 (1954)
- 3) Kon, T. : Trans. Jap. Soc. Civ. Eng. 5 (1950)
- 4) Sawada, M. : Part 1. Bull. Gov. For. Exp. Station Japan. 71 (1954)
- 5) Mori, T., Asano, I : Jap. Build. Res. Inst. Rep. 100 (1950), 144 (1951)
- 6) Sawada, M. : Part 2, Bull. Gov. For. Exp. Station, Japan. 71 (1954)

### 摘 要

使用した削片はSタイプ(長さ5cm,幅1.3mm,厚さ各0.28,0.61及び1.18mm,ブナ)及びRタイプ(長さ5cm,幅1.2cm,厚さ0.24mm,ヒノキ)の2種で前者には尿素系樹脂結合剤7.3%重量比,後者には6.5%を添加,比重0.4~1.1の範囲で熱圧成板した。

測定項目は比重,含水率,引張,圧縮並に剪断強度,引張及び圧縮弾性係数で試験片は第1図の如くである。

1,強度と比重との関係は第2図の如く指数曲線的で且つ削片厚の強度に与える影響は殆ど認められない(Sタイプ),特に注目すべき事は引張強度が圧縮強度より小さい事である。弾性係数と比重との関係も指数曲線的で(第3図)且つ引張,圧縮弾性係数はSタイプでは差異はないがRタイプでは比重0.7以上ではかなり異つて来る。本報告では以下両者等しいと仮定して考察を進める

こととする。強度と弾性係数の間には(1)式の如き関係が存在する。

2, 圧縮及び引張の応力—歪曲線は第5図の如くこの図から単一断面のビームに於ける応力分布は第6図となる。これは今<sup>3)</sup>の木梁の場合の引張, 圧縮側を逆にした場合に相当しその曲げ破損係数は極限の条件を若干変更すれば全く同様にして例えば単一中央集中荷重の場合それぞれ(2), (3), (4)式の如く求められ(2), (3)式及び(3), (4)式の適用限界の  $(h/l)_1$  及び  $(h/l)_p$  は(5)式により与えられる。第一表には数個の曲げ試験片について計算結果を示した, これによると  $h/l < (h/l)_1$  即ち曲げ破損は塑性域引張破損により生ずることとなり実験結果もこれに合致する。

3 プライの合成断面梁の場合単一断面に於ける応力分布曲線の単なる幾何学的組合せを用いることは疑義があるがここでは近似的に之を使用することとする。この場合の応力の進行過程は種々考えられるが(1)式の関係から第7図が重要と考えられる。これは沢田<sup>6)</sup>の集成材の場合の引張側と圧縮側とを交換し且つ極限条件を若干変更すれば全く同様にして例えば中央単一集中荷重の場合の曲げ破損係数(7), (8), (9)を得(6), (7)式の適用限界を示す  $(h/l)_1$  は(10)式となる。第2表にこの種のコンストラクションの曲げ試験片の計算結果を示す。タイプ1, 2共に  $h/l < (h/l)_1$  即ちビームは引張曲げ破損〔7(式)〕により破損することになるが実際には低比重(低剪断強度)のコアを用いたタイプ1では明かに剪断による曲げ破損を生じた。これは  $h/l$  と  $(h/l)_1$  の値が比較的接近していること, 実際に強度に若干のむらがあること等にもよるが反面前述の如く応力分布の単なる幾何学的組合せに基く誤差とも考えられる。最後にベニア・オーバーレイのサンドウイツチ・コンストラクションの場合木材及びチップ・ボードの引張, 圧縮強度と弾性係数の関係から第8図の如き2系列の応力分布の進行過程が考えられる。第1系列は低比重のチップ・ボード・コアに各種の厚さの単板, 又は中比重のコアに比較的厚い単板をオーバー・レイした場合に現われ第2系列は中比重のコアに薄単板をオーバー・レイした場合に屢々現われる。然し第2図の場合に比較して比重の割合に剪断強度の大きいチップ・ボードを使用する場合は第1系列は第2系列へと移行する故結局第2系列が重要となる。この場合の剪断応力分布曲線の計算は相当面倒であり, 又実用上塑性域引張破損による破損が多いと考えられる故ケース1の場合を除き塑性域引張曲げ破損係数のみを求めた。即ち例えば中央単一集中荷重のビームに於ける塑性域引張, 塑性域剪断, 弾性域剪断による各曲げ破損係数は夫々(13), (15)及び(16)式により与えられケース2, 3, 4に於ける塑性域引張曲げ破損係数は夫々(18), (19)及び(20)式により求められる。一例として比重0.65のチップ・ボード・コアに厚さ夫々0.5, 1.0, 1.5 mm 単板をオーバー・レイした場合の曲げ破損係数を求めて図示すると第14図の如くなる。即ちこの程度のチップ・ボード・コアでは0.5 mm 以下の単板をオーバー・レイしても強度的には無意味で1~1.5 mm が最も有効となる, これより厚さが増すとコアの剪断破損を生ずる様になり之又, 不適當となる。

本実験に協力された野口昌巳, 佐々木光, 杉本三千代の諸氏に感謝の意を表す。